

Axial-vector weak coupling at medium momentum for astro neutrinos and double beta decays

H. Ejiri

Research Center for Nuclear Physics, Osaka University, Osaka 567-0047, Japan

E-mail: ejiri@rcnp.osaka-u.ac.jp

Abstract. Neutrino nuclear responses associated with medium momentum transfer of $q=20-80$ MeV/ c for astro neutrinos and double beta decays (DBDs) were studied by using charge exchange (${}^3\text{He},t$) reactions on ${}^{128}\text{Te}$ and ${}^{130}\text{Te}$. Gamow-Teller and spin-dipole nuclear matrix elements (NMEs) are found to be reduced uniformly in the wide momentum region of $q=20 - 80$ MeV/ c with respect to pnQRPA NMEs by the coefficient of $k_{NM} \approx 0.35$, while the Fermi NME for the isobaric analogue state is given by the sum rule limit in the momentum transfer region. The reduction is discussed in terms of the quenching of the axial vector coupling g_A^{eff} for astro-neutrinos and DBDs. .

Key words: Axial weak coupling g_A , astro neutrinos, double beta decay, nuclear matrix element, momentum transfer, quenching of axial vector transitions, charge exchange reaction.

1. Introduction

Neutrino nuclear responses for astro neutrinos and double beta decays (DBDs) are crucial for studying neutrino properties of astro and particle physics interests. They are discussed in review articles and references therein [1, 2]. Recent works on DBD experiments and the nuclear matrix elements (NMEs) are given in reviews and references therein in

The neutrino response for the axial vector weak coupling is of current interest in views of possible renormalization (quenching) effect. The responses studied by $\beta - \gamma$ transitions at the low momentum transfer of $q \approx$ a few MeV/ c are reduced with respect to simple model evaluations. On the other hand the responses involved in supernova neutrinos and neutrino-less DBDs are associated with the medium momentum transfer of $q \approx 20-100$ MeV/ c .

The present work aims to study the momentum dependence of the axial-vector neutrino responses relevant to such astro neutrinos and DBDs by using charge exchange reactions (CERs), and to show that the renormalization (quenching) factors for the Gamow-Teller (GT) and spin-dipole (SD) responses are universal in the wide q -transfer region of $q=2-100$ MeV.

The neutrino (weak) nuclear response is expressed in terms of the weak coupling g_W and the NME $M(\alpha)$ for the α mode interaction as

$$g_W^2 B(\alpha) = g_W^2 (2J_i + 1)^{-1} |M(\alpha)|^2, \quad (1)$$

where J_i is the initial state spin, and g_W is the nucleon weak coupling with W being V for the vector coupling and A for the axial vector one. The interaction modes to be discussed in the present report are α =F (Fermi), GT and SD. The F and GT modes are involved mainly in low-energy astro neutrinos and the GT mode in the two neutrino DBDs. On the other hand the SD mode is also involved in the higher-energy supernova neutrinos and is one of the major components of the neutrino-less DBDs [8].

The weak couplings for the momentum transfer q are usually expressed by using the dipole approximation,

$$g_W = \frac{g_W^0}{(1 + q^2/M_W^2)^2}, \quad (2)$$

where g_W^0 is the weak coupling strength at zero momentum transfer ($q^2 = 0$), and M_W is the weak mass, respectively. For the vector and axial-vector masses one usually takes $M_V = 840$ MeV and $M_A \sim 1$ GeV [11, 12, 13] coming from the accelerator-neutrino phenomenology. In the present momentum region of $q \approx 20$ -100 MeV/c, the q dependence is very small, only of an order of 0.02 or less. Then one may assume constant g_W in the present momentum region. Then the q dependence of the response is considered to be mainly concerned with that for the NMEs $M(\alpha)$.

So far, the GT and SD responses (NMEs) have been studied experimentally by investigation β decays, electron captures (ECs) and γ decays, where the momentum transfer involved is as low as $q \leq$ a few MeV/c.

2. Charge exchange reactions on ^{128}Te and ^{130}Te

Recently high energy-resolution CER experiments of ($^3\text{He}, t$) have been studied for nuclei of astro-neutrino and DBD interests at RCNP Osaka University. as given in the review articles [2, 5, 7]. The Fermi, GT and SD responses are derived by analyzing the CERs in the angular range of $\theta=0$ -4 deg., corresponding to the momentum range of 5-120 MeV/c.

In the present work, we discuss F, GT and SD responses for even even nuclei with $J_i=0$. Then the spin factor is $2J_i+1=1$. The interaction operators are given as

$$T(F) = \tau^\pm, \quad T(GT) = \tau^\pm \sigma \quad T(SD) = \tau^\pm [i^1 \sigma \times f(r) Y_1]_2, \quad (3)$$

where τ and σ are the isospin and spin operators, respectively. The NMEs are given as $M(\alpha) = \langle T(\alpha) \rangle$ with α =F, GT, and SD. Actually, there are strong isospin and spin nuclear interactions, which are repulsive in nature, and thus the NMEs are much modified in nucleus due to nucleonic and non-nucleonic isospin spin correlations [2, 7].

Then the NME is given as

$$M(\alpha) = k_{NM}^{eff} M_{QR}(\alpha), \quad (4)$$

where $M_{QR}(\alpha)$ is the pnQRPA model NME and k_{NM}^{eff} stands for the re-normalization (quenching) coefficient due to all kinds of nuclear and non-nuclear correlation and nuclear medium effects, which are not explicitly included in the pnQRPA model NME.

Recent analyses of β^- and EC NMEs at the low-momentum transfer of $q \leq$ a few MeV/c show i. the F strength is concentrated in one isobaric analog state (IAS) and no strengths are located in the low-lying states, and ii. the GT and SD strengths at the low-excitation region are shifted up to the broad GT and SD giant resonances (GRs) at the high excitation region, and thus the GT and SD NMEs for low-lying states are reduced much from the simple quasi-particle pnQRPA NMEs $M_{QR}(\alpha)$ by the reduction factor of the order of $k_{NM}(\alpha) \approx 0.4-0.6$ partly due to the non-nucleonic $\tau\sigma$ correlations and nuclear medium effects [1, 2, 14, 15].

In the present report we discuss the q dependence of CERs on $^{128,130}\text{Te}$, which are of astro-neutrino and DBD interest, for the F (IAS), the lowest GT state and the lowest SD state in $^{128,130}\text{I}$ [17, 18]. The GT and SD states are mainly excitation of the single quasi-neutron to single quasi-proton states of the $2d(3/2)_n \rightarrow 2d(5/2)_p$ and the $1h(11/2)_n \rightarrow (1g7/2)_p$, while the F (IAS) state is the Fermi GR for the coherent $j = (l \pm 1/2)_n \rightarrow j = (l \pm 1/2)_p$ excitations.

The Q values of the CERs for the low-lying states are much smaller than the incident ^3He beam energy. Thus the momentum transfer is given by $q \approx P_i\theta$ with P_i and θ being the incident ^3He momentum and the out-going t angle.

The reaction diagram is schematically shown in Fig. 1.

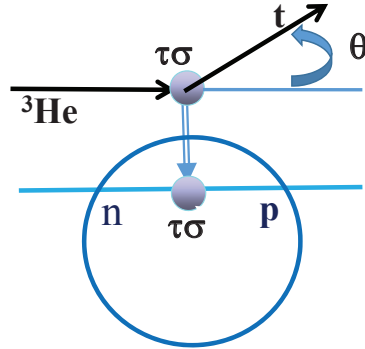


Figure 1. Schematic diagram of the $(^3\text{He}, t)$ for the isospin (τ) spin (σ) excitation. θ denotes the scattered angle of t .

In case of the RCNP beam energy of $E=0.42$ GeV, the differential cross sections in the medium momentum region of $q \approx 20-100$ MeV/c are measured by observing the angular distribution of t over $\theta=0-4$ deg.

The differential cross sections for them are derived as a function of the momentum transfer q from the observed angular distributions [17]. The obtained q distributions for the F, GT and SD states in ^{128}I and ^{130}I are shown, respectively, in Fig. 2 and Fig. 3.

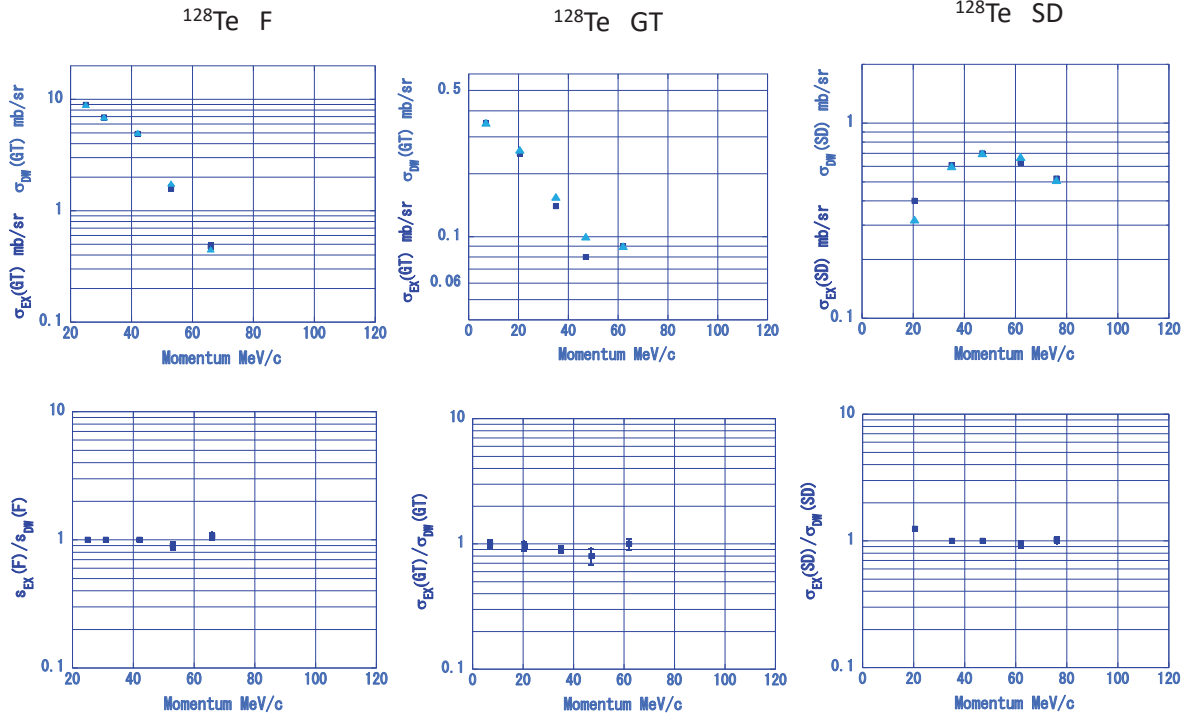


Figure 2. Top: The ^{128}Te ($^3\text{He},t$) CER cross sections as a function of the momentum transfer q . F, GT and SD stand for the 0^+ 8.31 MeV IAS, the 1^+ 0.12 MeV GT state, and the 2^- ground SD state, respectively. Squares: Experimental $\sigma_{EX}(\alpha)$. Triangles: DWBA $\sigma_{DW}(\alpha)$. Bottom: Squares: The ratio of the experimental to the DWBA cross sections as a function of the momentum transfer q for $\alpha = \text{F}$ (IAS), GT (1st GT), and SD (ground) states. See text.

The differential cross section for the α state is expressed as

$$\frac{d\sigma(\alpha)}{d\Omega} = K(\alpha)F(\alpha, q)J(\alpha)^2B(\alpha), \quad (5)$$

$$B(\alpha) = \kappa^{eff}(q)^2B^0(\alpha), \quad (6)$$

where $K(\alpha)$ and $J(\alpha)$ with $\alpha = \text{F}$, GT, and SD are the kinematic factors and the volume integrals of the interaction, respectively. The kinematic q -dependence is given by $F_i(\alpha, q)$. The q -dependent response is effectively expressed as $B(\alpha) = \kappa^{eff}(q)^2 B^0(\alpha)$ with $B^0(\alpha)$ being the nuclear response at $q=0$. The coefficient $\kappa^{eff}(q)$ stands for the effective q -dependent coupling. Accordingly, the NMEs are given as $M(\alpha) = \kappa^{eff}(q) M_i^0(\alpha)$ with $M_i^0(\alpha)$ being the NME at $q=0$.

The kinematic q -dependence $F_i(\alpha, q)$ is evaluated by the DWBA calculation. In the present case of the medium energy projectile, the distortion effect is rather small, and thus the kinematic factor is approximately given by the square of the spherical

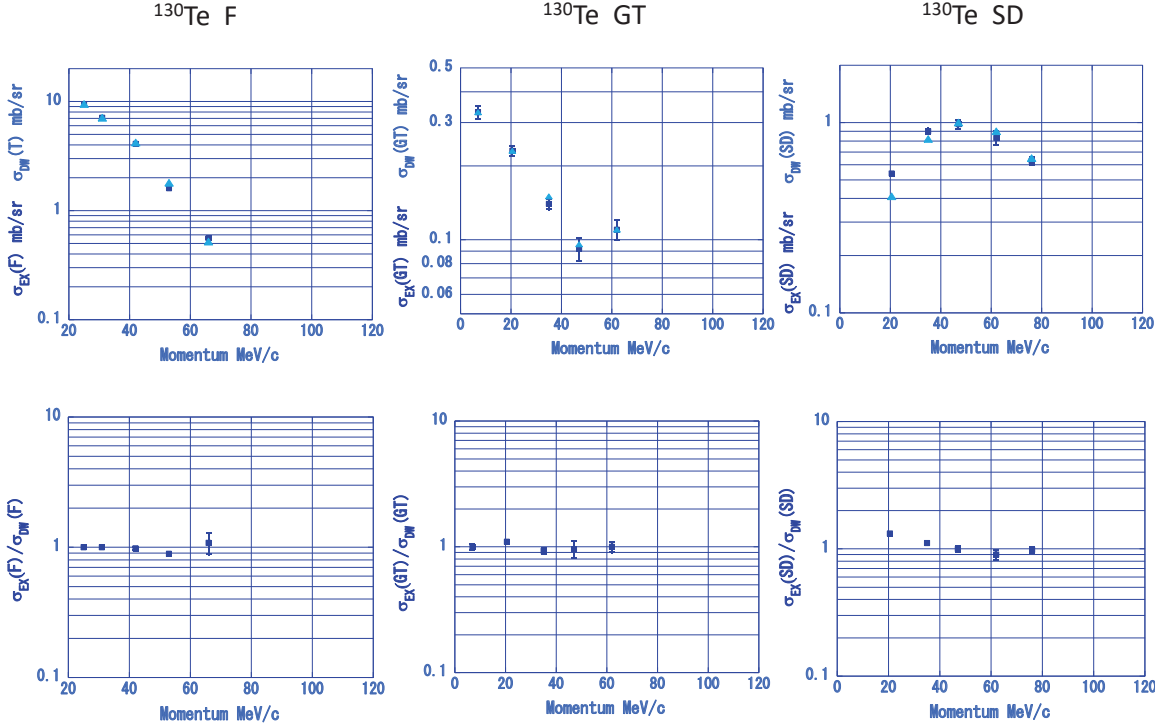


Figure 3. Top: The ^{130}Te ($^3\text{He},t$) CER cross sections as a function of the momentum transfer q . F, GT, and SD stand for the 0^+ : 12.72 MeV IAS, the 1^+ 0.12 MeV GT state and the 2^- ground SD state, respectively. The solid lines are the DWBA calculations. Squares: Experimental values. Triangles: DWBA values. Bottom: Squares: The ratio of the experimental to the DWBA cross sections as a function of the momentum transfer q for $\alpha = \text{F}$ (IAS), GT (1st GT), and SD (ground) states. See text.

Bessel function of $|J_l(qR)|^2$ with l being the orbital angular momentum transfer, and R being the effective interaction radius. The q -dependent coupling $\kappa^{eff}(q)$ manifests as deviation of the observed q (angular) distribution from the DWBA calculation. The observed q -dependences of the CER cross sections $\sigma_{EX}(\alpha)/d\Omega$ for $\alpha = \text{F}$, GT, and SD responses are well reproduced by the DWBA calculations $\sigma_{DW}(\alpha)/d\Omega$ with constant $\kappa^{eff}(q)^2$ as shown in Figs. 2 and 3.

The ratios of $\sigma_{EX}(\alpha)/d\Omega$ to the $\sigma_{DW}(\alpha)/d\Omega$ for ^{128}Te and ^{130}Te are also shown in Figs. 2 and 3. We note that the ratios are nearly 1 for the momentum region of the present interest. Accordingly the experimental distributions for F, GT, and SD components are well expressed by the DWBA ones with the kinematic q -dependent distribution and the constant coefficient for each $\kappa^{eff}(\alpha)$ for the $\alpha = \text{F}$, GT, and SD NMES over the momentum region of $q = 30\text{--}80$ MeV/c .

Actually, the observed and DWBA q -distribution for the 0^+ F (IAS) states consists

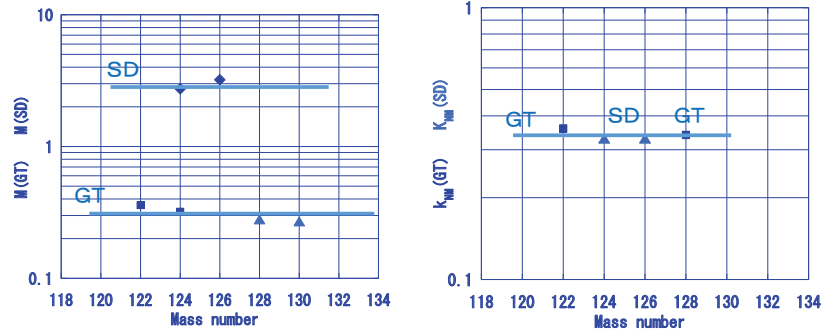


Figure 4. Left side panel: NMEs for GT and SD transitions in Te isotopes. Squares triangles and diamonds are the GT NMEs from β/EC decays, the GT NMEs from CERs and the SD NMEs in units of 10^{-3} n.u. from the β/EC decays, respectively. Right side panel: Re-normalization (quenching) coefficients for GT and SD NMEs. Squares and triangles are the values for the GT β/EC and the SD β/EC decays, respectively. See text.

of the pure $l=0$ component, while those for the 1^+ GT ($l=0$) include the admixture of the $l=2$ component beyond the momentum $q \geq 40$ MeV, and those for the 2^- SD ($l=1$) state include the admixtures of the $l=3$ component beyond the momentum $q \geq 60$ MeV. In other words, the good agreement of the experimental and DWBD q distributions in the wide momentum region of $q=10-80$ MeV/c, which is relevant to the angular momentum transfers of $l=0-3$ suggest the universal quenching coefficients over the wide linear and angular momentum regions of the astro and DBD interests. The present results are in accord with the discussion on ^{76}Ge in the review [3].

3. Quenching of the axial-vector weak coupling

The GT and SD NMEs at the low q (\leq a few MeV) region for DBD and other medium-heavy nuclei are experimentally available from the β/EC data. They are reduced with respect to the pnQRPA NMEs by the coefficient $k_{NM}(0) \approx 0.35-0.65$ at the β/EC point of $q \approx 0$ [14, 15]. The experimental GT and SD NMEs in the Te isotopes are shown in the left panel of Figure 4, and the re-normalization (quenching) coefficients for the GT and SD NMEs with respect to the QRPA NMEs are shown in the right panel. They are quite uniform in the mass region of $A=122-130$. Thus the axial-vector weak coupling is considered to be uniformly re-normalized (quenched) by the coefficient $k_{NM}(q) \approx 0.35$ in the wide momentum region of $q=0-80$ MeV/c, which is the region of the neutrino-less DBDs and medium-energy supernova neutrinos.

The present work shows the axial-vector GT and SD NMEs are reduced (quenched) with respect to the pnQRPA NMEs in the wide momentum region of the neutrino-less DBD and super-nova neutrino interest as seen in the GT and SD NMEs at the low momentum region found in the β/EC decays [14, 15]. The NMEs studied in the present

Table 1. Experimental and pnQRPA GT and SD NMEs at $q \approx$ a few MeV for Te isotopes. SD NMEs are in unit of 10^{-3} n.u. See refs.[14,15]. k_{NM}^{eff} : effective reduction factor. See tex

Transition	α	$M_{EX}(\alpha)$	$M_{QR}(\alpha)$	k_{NM}^{eff}
$^{124}\text{Te} \leftrightarrow ^{124}\text{I}$	GT	0.36	0.99	0.36
$^{126}\text{Te} \leftrightarrow ^{126}\text{I}$	SD	2.743	8.38	0.33
$^{128}\text{Te} \leftrightarrow ^{128}\text{I}$	SD	3.22	9.62	0.33
$^{130}\text{Te} \leftrightarrow ^{130}\text{I}$	GT	0.32	0.90	0.34

CERs are the τ^- -side NMEs.

The τ^+ -side neutrino response has recently been studied by ordinary muon capture (OMC) reaction [19, 20, 21]. The axial-vector NMEs in the similar momentum region of $q=50-100$ MeV/c are found to be reduced by the re-normalization coefficient of $k_{NM} \approx 0.4$ with respect to the pnQRPA NMEs. [19, 21]. Then, one may expect the DBD NMEs are reduced by a re-normalization coefficient around $k_{NM} \approx 0.3-0.4$ with respect to the pnQRPA NMEs, depending on the relative weight of the axial-vector NME.

The supernova neutrino is in the medium momentum region of 10-50 MeV/c. Then the NME for the axial vector transition is given by

$$M^\nu = k_{NM} M_{QR}^\nu(\alpha), \quad (7)$$

where $k_{NM} \approx 0.3-0.4$ is the re-normalization (quenching) coefficient and $M_{QR}^\nu(\alpha)$ is the pnQRPA NME. Then the interaction rate is reduced by the coefficient of $(k_{NM})^2 \approx 0.1-0.2$ with respect to the pnQRPA rate for the wide q region.

The neutrino-less DBD NME is given by

$$M^{0\nu} = (k_{NM}^{eff})^2 [M_{GT}^{0\nu} + M_T^{0\nu}] + M_F^{0\nu}, \quad (8)$$

where $M_{GT}^{0\nu}$, $M_T^{0\nu}$ and $M_F^{0\nu}$ are the axial-vector, tensor, and vector DBD NMEs, respectively. Then the axial-vector and tensor NMEs are reduced with respect to the pnQRPA NMEs by the re-normalization (quenching) coefficient of $(k_{NM}^{eff})^2 \approx 0.1-0.2$, and the DBD NME by the re-normalization (quenching) coefficient of 0.15-0.3, depending on the relative weight of the vector NME with respect to the axial-vector + tensor NMEs. Then the DBD isotope (detector) mass required for a given ν -mass sensitivity is 2-3 orders of magnitude more than the detector mass in case of the pnQRPA NME.

In case of the two neutrino $\beta\beta$ NMEs, the matrix element is given by the product of the τ^- -side and τ^+ -side GT NMEs at the low $q=0-3$ MeV/c. Thus the two-neutrino NMEs are found to be reduced by the coefficient $k \approx k^- \times k^+$ with k^\pm being the reduction coefficient for the τ^\pm GT NMEs [3, 22, 23]. Accordingly, the axial-vector DBD NME might be reduced by the similar coefficient.

It is noted that the re-normalization (quenching) coefficient k_{NM} is conventionally expressed as g_A^{eff}/g_A . It is very interesting to evaluate theoretically the re-normalization coefficient by taking into accounts all kinds of nuclear medium and non-nucleonic cor-

relation effects, which are not explicitly included in the pnQRPA model.

The author thank Prof. J. Suhonen for valuable discussions.

References

- [1] Ejiri H 1978 *Phys. Report* **38** 85
- [2] Ejiri H 2000 *Phys. Rep.* **338** 265
- [3] Ejiri H, Suhonen J and Zuber Z 2019 *Phys. Rep.* **797** 1.
- [4] Suhonen J and Civitarese O 1998 *Phys. Rep.* **300** 123.
- [5] Ejiri H 2005 *J. Phys. Soc. Jpn.* **74** 2101
- [6] Avignone F, Elliott S and Engel J 2008 *Rev. Mod. Phys.* **80** 481
- [7] Vergados J, Ejiri H and Šimkovic F 2012 *Rep. Prog. Phys.* **75** 106301
- [8] Suhonen J and Civitarese O (2012) *J. Phys. G: Nucl. Part. Phys.* **39** 124005.
- [9] Vergados J, Ejiri H and Šimkovic F 2016 *Int. J. Mod. Phys. E* **25** 1630007
- [10] Engel J and Menendez J 2017 *Rep. Prog. Phys.* **60** 046301.
- [11] Bodek A, Avvakumov S, Bradford R and Budd H 2008 *Eur. Phys. J. C* **53** 349–354.
- [12] Bhattacharya B, Hill R J and Paz G (2011) *Phys. Rev. D* **84** 073006.
- [13] Amaro J E and Arriola E R 2016 *Phys. Rev. D* **93** 053002..
- [14] Ejiri H and Suhonen J 2015 *J. Phys. G* **42** 055201.
- [15] Ejiri H, Soukouti N, Suhonen J 2014 *Phys. Lett. B* **729** 27
- [16] Suhonen J 2017 *Phys. Rev. C* **96** 05501.
- [17] Puppe P *et al.* 2012 *Phys. Rev. C*, **86** 044603.
- [18] Ejiri H and Frekers D 2016 *J. Phys. G Nucl. Part. Phys.* **43** 11LT01.
- [19] Hashim I.H, Ejiri H, Shima T, Takahisa K, Sato A, Kuno Y, Ninomiya K, Kawamura N, and Miyatake Y 2018 *Phys. Rev. C* **97** 014617.
- [20] Zinatulina D, *et al.* 2019 *Phys. Rev. C* **99** 024327.
- [21] Jokiniemi L, Suhonen H, Ejiri H, and Hashim I.H. 2019 *Phys. Lett. B* **794** 143.
- [22] Ejiri H 2009 *J. Phys. Soc. Jpn.* **78** 074201.
- [23] Ejiri H 2012 *J. Phys. Soc. Jpn. letters.* **81** 033201.